e-ISSN: 2550-164X

Available online at
https://jmeche.uitm.edu.my/

Journal of Mechanical Engineering 23(1) 2026, 1 – 18.

Journal of Mechanical Engineering

Optimization of 3D Printing Parameters for Strength Enhancement of PLA Notched Curved Panels using Taguchi Method

Abdul Malik Hussein Abdul Jalil[1*], Wahyu Kuntjoro[1], Rizal Effendy Mohd Nasir[2], Juri Saedon[2]

[1]*Caidmark Sdn Bhd, Shah Alam, Selangor, Malaysia*
[2]*Faculty of Mechanical Engineering, Universiti Teknologi MARA (UiTM), Shah Alam, Selangor, Malaysia*

ARTICLE INFO

Article history:
Received 07 January 2025
Revised 29 July 2025
Accepted 02 August 2025
Online first
Published 15 January 2026

Keywords:
Taguchi
Design of experiment
Optimization
Plate with hole
PLA

DOI:
10.24191/jmeche.v23i1.4574

ABSTRACT

Prototypes and components are increasingly printed using 3D printing. 3D printing issues depend on component shape and material. How 3D printing is done always affects structural component properties. Contemporary structural components, especially in small, unmanned planes, use 3D-printed curved panels with notches. This paper optimised 3D printing parameters to find the strongest notched curve panel using the Taguchi experimental design. PLA was used. The method involved 3D printing notched curve specimens with dimensions of 200 × 80 × 1.8 mm and a fixed notch diameter of 40 mm. Notched panel curve radius is 800 mm. Creality CR10S Pro-V2 3D printer printed the specimens. Three specimens were created for each configuration, utilising 3D printing parameters: printing direction, nozzle temperature, printing speed, layer thickness, and infill percentage, which were identified through literature reviews. The specimens were tested for strength using the universal testing equipment after printing. After collecting test data, the Taguchi design of experiment was used to determine the best process parameters. Specimen with configuration number five (5), printing direction 90°, nozzle temperature 195 °C, printing speed 60 mm/s, layer thickness 0.2 mm, and infill percentage 100%, produced the highest strength. Analysis of variance (ANOVA) and S/N ratio response validated this conclusion. The formula 'larger-the-better' showed that printing direction had the highest S/N Ratio (8.2659). Printing direction, nozzle temperature, and speed contributed 55%, 27%, and 8%, respectively, to the process optimisation, according to ANOVA. Taguchi design of experiment can optimise the 3D printed notched curve shell for strength.

[1*] Corresponding author. *E-mail address*: abdulmalikhussein@gmail.com
https://doi.org/10.24191/jmeche.v23i1.4574

INTRODUCTION

Rapid prototyping gave birth to 3D printing methods with enormous potential (Siraj & Bharti, 2020). 3D printing is also known as additive manufacturing due to its process. During 3D printing, material layers are added one by one, following the CAD geometry shape that has been specified. The Fused Deposition Modelling (FDM) technique will be used for this research. FDM was introduced in 1988 by Scott Crump, the founder of Stratasys (Liu et al., 2014). This technique utilizes a heated FDM head that prints out the material onto a heated bed, following the geometry shape created in the CAD software. 3D printing can be used in a variety of ways. The technology can be used to 3D print shaped curved panels or shells to develop aircraft models (Iljaszewicz et al., 2020). Besides this, 3D printing technology also applies to various industries, such as electronic and control systems such as a series of representative electronic patterns spanning from single wires to desired complex configurations such as integrated circuit (IC), printed-circuits-on-board (PCB), electronic paintings, or more do-it-yourself (DIY) devices, was demonstrated to be printed out with high precision in a moment (Zheng et al., 2014a). In automotive, various internal components can be 3D printed (Michaels, 2017). In the aircraft industry, Boeing is looking at 3D printing lightweight titanium parts that could save them millions of dollars, such as structural components designed to bear the stress of an airframe in flight (Reuters, 2017). Further studies have been carried out on a 3D-printed sub-wing box lug joint assembly (Kuntjoro et al., 2022a) and a 3D-printed UAV straight wing box (Kuntjoro et al., 2022b). In the biomedical industry, 3D printing technology was used in developing artificial ears, such as bionic ear components (Mannoor et al., 2013), ceramic and glass (Nguyen et al., 2017) and metamaterials such as the production of these micro lattices, with constituent materials ranging from polymers to metals and ceramics, is made possible by using projection micro stereolithography, an additive micromanufacturing technique, combined with nanoscale coating and post-processing (Zheng et al., 2014b).

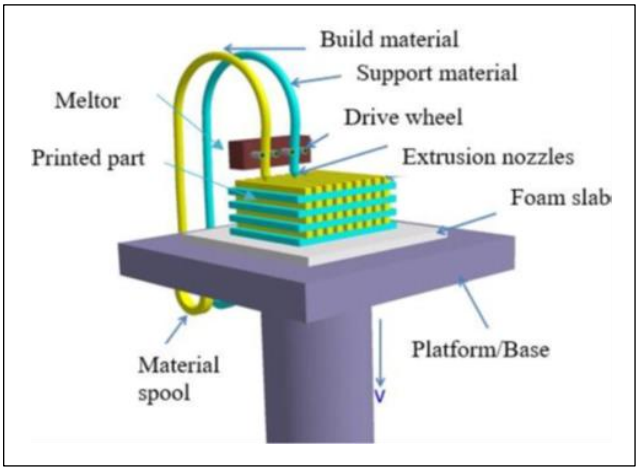

Fig. 1. Schematic diagram of FDM printer.

Fig 1 describes the schematic diagram of the FDM printer (Kumar & Kumar, 2020). The bed moves in the z direction while the head printer moves in the x and y directions (Dave et al., 2022). The filament is fed through a heater (extruder) built into a printer head before being deposited semi-molten through a nozzle. Motor-covering moves the flatbed and head, and the slicing software sets the relative movement between the two. The model is first constructed in 2D by the printer, which is then raised to increase the space between the nozzle tip and the bed so that the next layer can be applied. The machine continues this way until the entire 3D model has been created (Aloyaydi et al., 2019).

https://doi.org/10.24191/jmeche.v23i1.457

The FDM process of 3D printing is becoming more popular. The process is easy to use, has a low-cost setup, can produce prototypes and tooling, has higher dimensional stability, uses inexpensive equipment, consumes little power, and is portable. FDM printers also offer excellent dimensional stability and operate at lower temperatures (Bhavar et al., 2017; Chohan & Singh, 2017; Kun, 2016; Mohamed et al., 2015). The stress behaviour of a 3D-printed PLA plate with a hole was also investigated (Kuntjoro et al., 2023a).

This paper focuses on three (3) aspects. The first aspect is the fabrication of a 3D object specimen that will be used for testing. This feature tests the 3D model creation by requiring it to apply the correct 3D printing procedure to 3D print a notched curved shell. The second aspect of this paper is that the specimen will be tested for strength using the universal testing machine. The third aspect of this paper is to calculate the optimum process parameters in 3D printing using the Taguchi design of the experiment method. This statistical method was first developed by Taguchi and Konishi (Athreya & Venkatesh, 2012). Originally designed to improve the quality of manufactured items (manufacturing process development), it has now been used in a wide range of engineering domains, including biotechnology (Rao et al., 2008).

The key advantages of utilizing Taguchi's technique for designing experiments are simplifying the experimental plan and the feasibility of studying interactions among different parameters (Anitha et al., 2001). The orthogonal array limits the number of tests to a manageable quantity in cost and time.

This study aims to find the optimum process parameters that can achieve the maximum strength of a 3D-printed notched curved shell. The reason for this is that plate structures with holes are commonly used in aerospace structures (Kim & Park, 2020; Mo et al., 2019). There are holes in a lot of the panels in the wing structures (Pukale & Reddy, 2014). Figs 2(a) and 2(b) depict an aircraft wing panel (Sundaresan et al., 2003). Historically, 3D printing has been widely used in the aerospace industry to create prototypes instead of structural engineering components (Guduru & Srinivasu, 2020). Increasing 3D printing's ability to create dependable engineering components for those applications is a major goal in industrial use (Ngo et al., 2018). Intricate geometry can be turned into a physical model with the help of 3D printing technology (Raj et al., 2018), and it is also capable of preparing near-net shaping of components (Cariapa et al., 2008; Tong et al., 2020). The study of 3D printing of notched curve shells is limited, while recent studies (Kuntjoro et al., 2023b; Muta'ali et al., 2020) have shown that these can be applied to various studies of aircraft design and analysis.

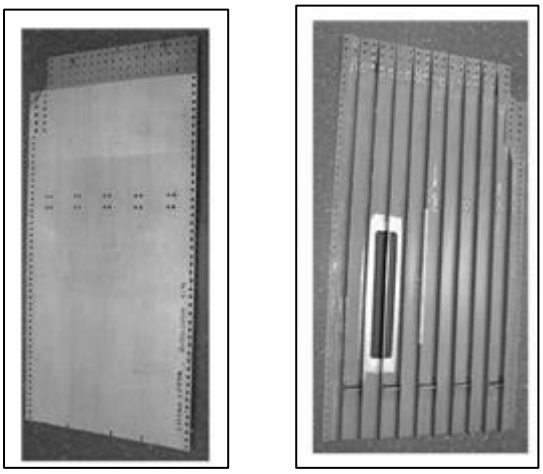

(a) (b)

Fig. 2. (a) Aircraft wing panel external and (b) internal views.

https://doi.org/10.24191/jmeche.v23i1.457

SETUP AND METHODOLOGY

This study consists of four (4) main phases. The first phase is to 3D print the required PLA notched curve samples using the fused deposition modelling (FDM) technique. The second phase is to reduce the number of samples to be analysed using the Taguchi design of the experiment method. The third phase of this study is to conduct the tensile strength testing on the samples using the universal testing machine. The fourth phase of this study is to identify the process by which the highest value of the strength can be obtained.

The samples in this study were 3D printed using the Creality 3D CR10S Pro-V2 printer. The 3D CAD model was developed using the Siemens NX CAD software. The Ultimaker Cura 4.11.0 was used to prepare the model for printing. Figs 3 and 4 show the samples' CAD model dimensions to be 3D printed and developed using the Siemens NX CAD software. As seen in Fig 3 and Fig 4, the center part of the sample is curved, making it a curved, notched shell, which is the novelty of this study.

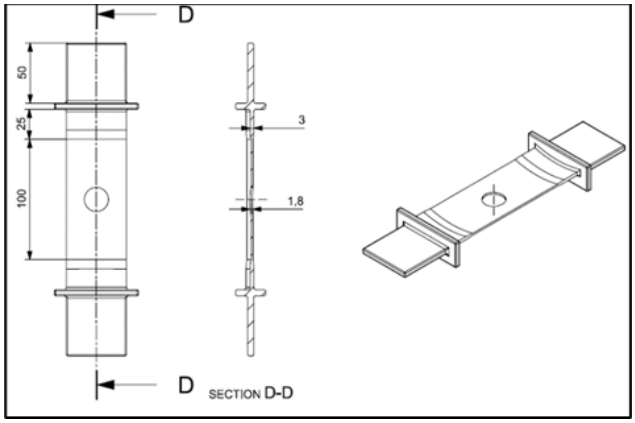

Fig. 3. Sample CAD model dimensions (view A).

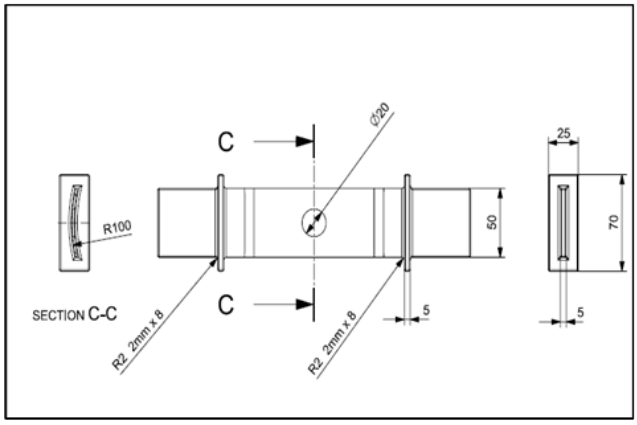

Fig. 4. Sample CAD model dimensions (view B).

Figs 5 and 7 show the CAD Model sliced in preparation for the 3D printing in 0° and 90° directions. This is done by using the Ultimaker Cura software. Other parameters include nozzle temperature, printing speed, layer thickness, and infill percentage. Here, the STL file format of the CAD model was converted to the G-code format as input for the 3D printer. Figs 6 and 8 show the sample being 3D printed using the

https://doi.org/10.24191/jmeche.v23i1.457

Creality 3D printer in 0° and 90° directions. The appearance of the holes in the specimen affects the printing quality, as the 3D printer prints the specimen layer by layer, compared to a solid-continuous sample. The holes created an irregular motion of the 3D printer nozzle, affecting the quality of the 3D printed specimen. Fig 9 shows the final 3D-printed sample.

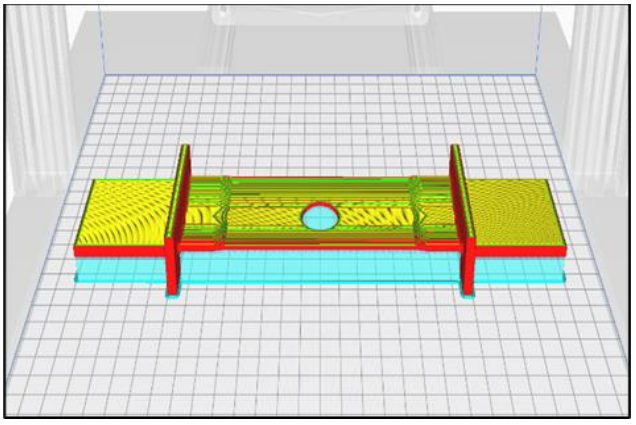

Fig. 5. Slicing the CAD model at 0° printing direction.

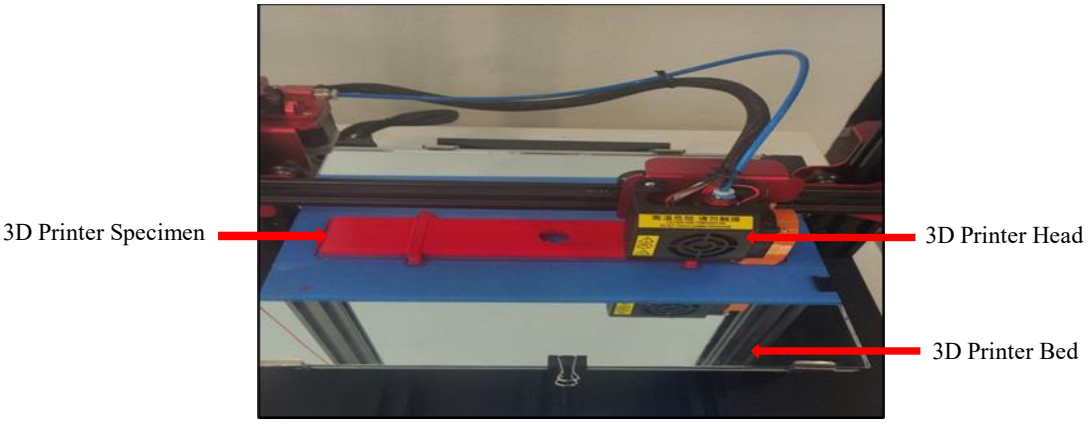

Fig. 6. 3D printing the sample at 0° printing direction.

https://doi.org/10.24191/jmeche.v23i1.457

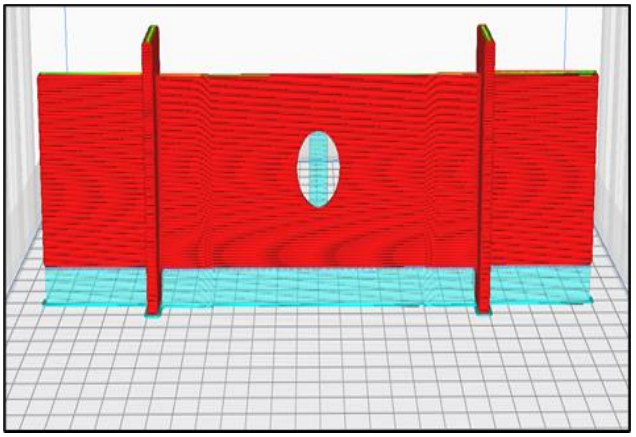

Fig. 7. Slicing the CAD model at 90° printing direction.

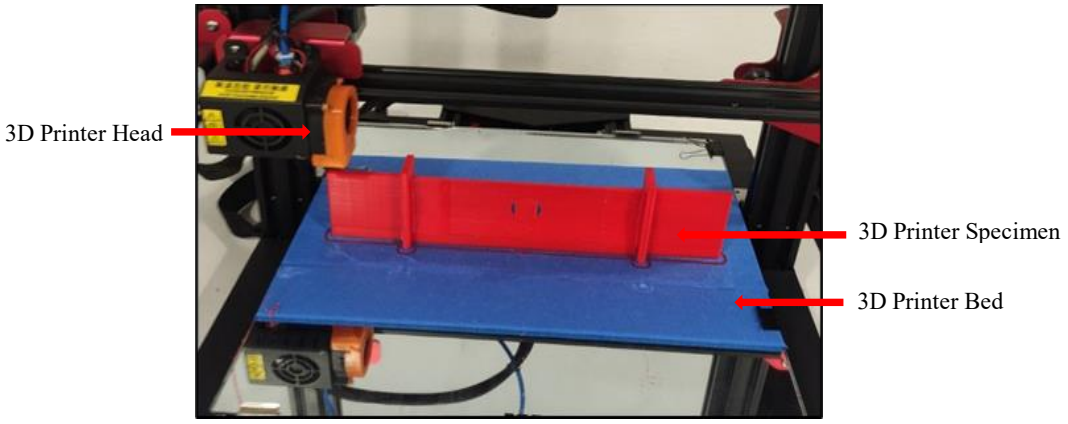

Fig. 8. 3D printing the sample at 90° printing direction.

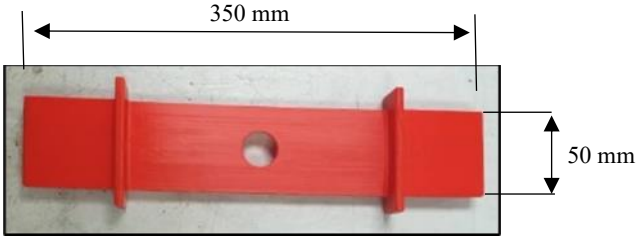

Fig. 9. 3D printed specimen.

Table 1 shows the 3D printing process parameters affecting the 3D printing specimens. In achieving a high finishing quality in 3D printing processes, it is also essential to understand the process parameters that influence the 3d printing of a particular design. This issue was explored to investigate the strength of test specimens that were 3D printed with different printing orientations according to the ISO 527-2-2012 standard (Yao et al., 2019). These parameters were chosen to provide a variety of orientations for testing purposes. These test specimens were printed with a three-layer thickness (0.1 mm, 0.2 mm, and 0.3 mm) at each angle with orientations of 0°, 15°, 30° 45°, 60°, 75°, and 90°. Theoretical and experimental data were

https://doi.org/10.24191/jmeche.v23i1.457

compared and found to agree. It was concluded that the specimen's strength was reduced as the layer thickness increased from 0.1 mm to 0.3 mm. Another study presented an intensive investigation of the effects of 3D printing temperature profile, such as an analysis of temperature and crystallization properties on the market, on two commercially available PLA (PLA 3d570 and PLA 3d870) (Schiavone et al., 2020). Different printing angles (0° and 90°) and infill patterns (line and gyroid) were selected. It was concluded that significant differences were obtained in the thermal profiles compared to other samples' printing sequences. Other research activities have given insights into the process parameters that can influence the 3D printing objects (Carlier et al., 2019; Dev & Srivastava, 2020; El Magri et al., 2020). The influence of infill pattern and layer thickness on the mechanical strength of PLA material in 3D printing technology was also investigated (Cho et al., 2019). It was concluded in another study that the process parameters, such as layer thickness, infill deposition speed, infill density, infill pattern, and infill width, had impacted the mechanical properties of the 3D printed specimens (Suteja & Soesanti, 2020).

Table 1. Process parameters that affect the 3D printing of the specimens

Process parameters	Noise parameters
Printing direction	3D print finishing quality
Nozzle temperature	-
Printing speed	-
Layer thickness	-
Infill percentage	-

It can be concluded that five (5) significant process parameters shall be considered for this study. They are printing direction, nozzle temperature, printing speed, layer thickness, and infill percentage, as described in Table 1. Table 2 illustrates the selected process parameters and their levels.

Table 2. Selected process parameters and their levels

Process parameters	Level 1	Level 2
Printing direction	0°	90°
Nozzle temperature	195 °C	240 °C
Printing speed	30 mm/s	60 mm/s
Layer thickness	0.2 mm	0.4 mm
Infill percentage	50%	100%

Noise parameters in Taguchi are defined as external factors that cannot be controlled. This study's noise parameter factor is the 3D print finishing quality, as at this stage, we did not control the surface quality. It can be further explained that each specimen that is 3D printed will have its surface finish, which affects its strength, and this factor is addressed by 3D printing three (3) samples per configuration, where average values of the strength were obtained. Three (3) samples are selected based on the resources and time.

The parameter setting is based on what can be manipulated in the 3D printer (Sheoran & Kumar, 2020). These are the extreme parameters so that significant results can be obtained. The number of levels gives the total number of experiments to be conducted to the power of the process parameters. In this case, $2^5 = 32$ experiments for an entire factorial experiment. The configurations of experiments are stated in Table 3.

https://doi.org/10.24191/jmeche.v23i1.457

Table 3. Experiment configurations run for full factorial

No	Printing direction (°)	Nozzle temperature (°C)	Printing speed (mm/s)	Layer thickness (mm)	Infill percentage (%)
1	0	195	30	0.2	50
2	0	195	30	0.2	100
3	0	195	30	0.4	50
4	0	195	30	0.4	100
5	0	195	60	0.2	50
6	0	195	60	0.2	100
7	0	195	60	0.4	50
8	0	195	60	0.4	100
9	0	240	30	0.2	50
10	0	240	30	0.2	100
11	0	240	30	0.4	50
12	0	240	30	0.4	100
13	0	240	60	0.2	50
14	0	240	60	0.2	100
15	0	240	60	0.4	50
16	0	240	60	0.4	100
17	90	195	30	0.2	50
18	90	195	30	0.2	100
19	90	195	30	0.4	50
20	90	195	30	0.4	100
21	90	195	60	0.2	50
22	90	195	60	0.2	100
23	90	195	60	0.4	50
24	90	195	60	0.4	100
25	90	240	30	0.2	50
26	90	240	30	0.2	100
27	90	240	30	0.4	50
28	90	240	30	0.4	100
29	90	240	60	0.2	50
30	90	240	60	0.2	100
31	90	240	60	0.4	50
32	90	240	60	0.4	100

Average results were obtained to address the noise parameters described in Table 1. The Taguchi design of the experiment method was used to reduce the number of experiments to save time and cost (Saedon et al., 2015). Taguchi's techniques use the Degree of Freedom (DOF) method to determine the number of experimental runs. DOF refers to the number of ways a system can independently be varied when a constant is imposed and can be described below.

$$Total\ Degrees\ of\ Freedom = \sum_{i=1}^{k}(S_k - 1) \quad (1)$$

$$Total\ Number\ of\ Experiments = 1 + Total\ Degree\ of\ Freedom \quad (2)$$

https://doi.org/10.24191/jmeche.v23i1.457

Table 4. Calculating the total degrees of freedom (DOF)

Process parameters	Total levels (S)	Degrees of Freedom (DOF=S-1)
Printing direction	2	1
Nozzle temperature	2	1
Printing speed	2	1
Layer thickness	2	1
Infill percentage	2	1
Total DOF		5

From Equation 2, it can be defined that the total number of experiments is six (6). In the Taguchi method, the orthogonal array selected shall be larger than or equal to the number of experiments calculated. As shown in Table 4, the L8 orthogonal array was established in this study and was presented in the results section. Next was preparing the samples for the universal tensile strength test using the universal strength testing machine.

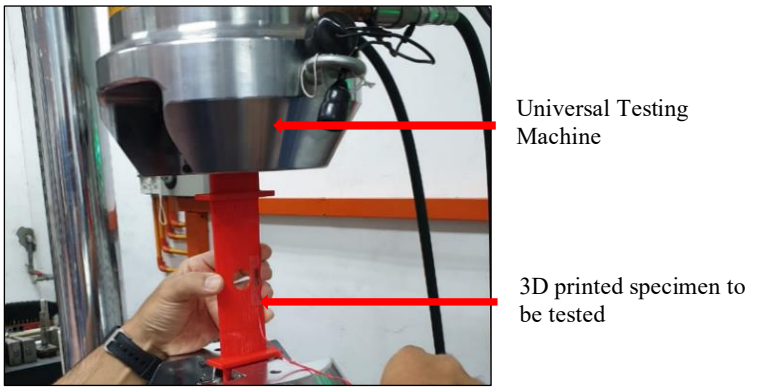

Fig. 10. Tensile testing on 3D printed specimen.

Fig 10 shows the tensile testing on the 3D-printed specimen. Once the results of these experiments have been obtained, the next step is to find the optimum process parameters that can fulfil the highest strength criteria using Equation (3).

$$S/N\ ratio = -10\ log_{10}\left(\frac{1}{n}\right)\sum_{i=1}^{n}\left(\frac{1}{y2ij}\right)\ \text{“larger the better”} \quad (3)$$

RESULTS AND DISCUSSION

This section summarizes and discusses the main findings of the work. Fig 11 shows where the 3D specimen failed during the stress test. Due to the shape and reduced area of the specimen around the hole, the failure occurred at the smallest net area with a significant stress concentration at the hole's edge. An experimental investigation of the effect on the specific strength of FDM fabrication using the ASTM D638 standard shows that failure is likely to occur in a similar specimen area (Iriç, 2020). In this study, the shape and size of the specimen are different from the ASTM D638 standard. This is because the nature of this study is to provide a curved shape for testing.

https://doi.org/10.24191/jmeche.v23i1.457

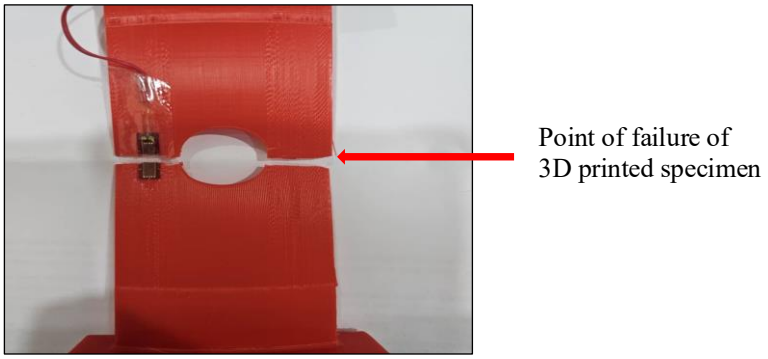

Fig. 11. Failure of the 3D-printed specimen.

As mentioned above, the L8 orthogonal array was selected per the Taguchi method (Munprom & Limtasiri, 2019), meaning eight (8) experimental configuration runs were selected and presented in Table 5.

Table 5. L8 orthogonal array

Configuration Number	Printing direction (°)	Nozzle temperature (°C)	Printing speed (mm/s)	Layer thickness (mm)	Infill percentage (%)
1	0	195	30	0.2	50
2	0	195	30	0.4	100
3	0	240	60	0.2	50
4	0	240	60	0.4	100
5	90	195	60	0.2	100
6	90	195	60	0.4	50
7	90	240	30	0.2	100
8	90	240	30	0.4	50

Experiments were carried out as per the eight (8) configurations above, three samples per configuration, and the results obtained for the average strength are shown in Table 6. The experiment was repeated twice per specimen (configuration number). The total number of experiments done was twenty-four (24). Fig 12 shows the strength plot with error bars.

Table 6. Average strength results

Configuration Number	Average strength (kN)	Average SD (kN)
1	2.37	0.21
2	2.36	0.3
3	2.32	0.16
4	2.33	0.14
5	2.59	0.06
6	2.54	0.05
7	2.39	0.05
8	2.42	0.08

https://doi.org/10.24191/jmeche.v23i1.457

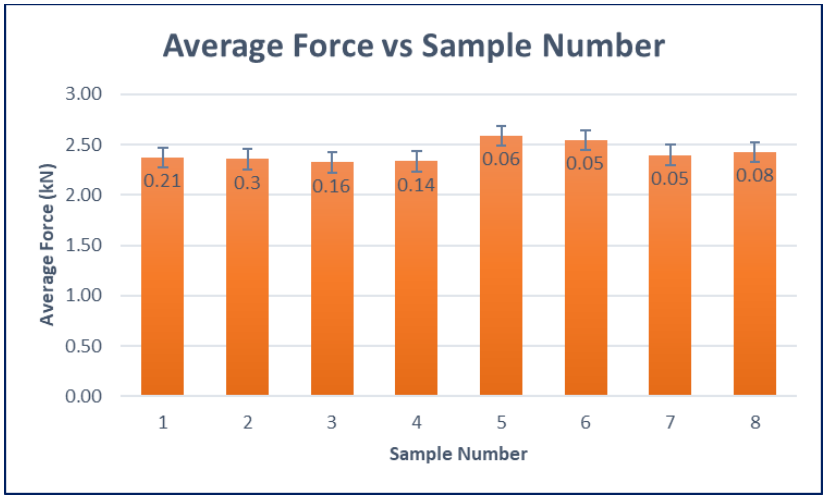

Fig. 12. Strength plot with error bars.

Table 6 shows that the highest strength value is at configuration no. 5, which is averaged at 2.59 kN. Average standard deviations are also presented. Configuration 5 process parameters are printing direction 90°, nozzle temperature 195 °C, printing speed 60 mm/s, layer thickness 0.2 mm, and infill percentage 100%. It can be said that 3D printing the specimen at 90° (axial) would exhibit a higher strength than 3D printing at 0° (lateral), as shown in Figs 6 and 8. Studies have shown that the printing direction affects the specimen strength, given the different orientations in which the specimens were printed (Yao et al., 2020). Other significant factors that influence the 3D printing of the specimen, such as nozzle temperature, infill percentage, and layer thickness, are further discussed in this study (Yadav et al., 2020).

From here, these experimental results are fed into the Minitab software to check for configurations that could give higher strength values. Here, the larger the better signal-to-noise ratio is applied. Table 7 displays the calculated S/N Ratio results for strength. It demonstrates that the strength ranges from 2.32 kN to 2.59 kN, with Test 5 having the highest strength at 2.59 kN. Printing direction (A) has the most significant values on increasing strength, as Table 8's S/N ratio table of strength response makes evident. Larger-the-better references were used to calculate S/N ratios; a parameter that received a ranking of one indicates that it has caused the largest strength in each experiment. It demonstrates that the printing direction parameter has had the greatest influence on increasing strength. As seen in Fig 13, the main effect plot of the S/N ratio clearly displays the impact of each parameter. Out of all the experiments, Test 5 exhibits the highest strength value (2.59 kN) and the highest S/N Ratio. $A_5B_5C_5D_5$ (printing direction = 90°, nozzle temperature = 195 °C, printing speed = 60 mm/s, layer thickness = 0.2 mm, and infill percentage = 100%) was the optimal level parameter value combination.

The analysis of variance (ANOVA) table for strength is displayed in Table 9. It demonstrates that the parameters of printing direction (55%), nozzle temperature (27%), and printing speed (8%) contributed significantly. It was a similar finding stated by Hikmat et al. (2021) and Yao et al. (2020) where printing direction is the most significant influence parameter.

https://doi.org/10.24191/jmeche.v23i1.457

Table 7. Strength results and S/N Ratios

Test No.	Printing direction (A)	Nozzle temperature (B)	Printing speed (C)	Layer thickness (D)	Infill percentage (E)	Average strength (kN)	Strength S/N Ratio
1	0°	195 °C	30 mm/s	0.2 mm	50%	2.37	7.4949
2	0°	195 °C	30 mm/s	0.4 mm	100%	2.36	7.4582
3	0°	240 °C	60 mm/s	0.2 mm	50%	2.32	7.3097
4	0°	240 °C	60 mm/s	0.4 mm	100%	2.33	7.3471
5	90°	195 °C	60 mm/s	0.2 mm	100%	2.59	8.2659
6	90°	195 °C	60 mm/s	0.4 mm	50%	2.54	8.0966
7	90°	240 °C	30 mm/s	0.2 mm	100%	2.39	7.5679
8	90°	240 °C	30 mm/s	0.4 mm	50%	2.42	7.6763

Table 8. Strength response table of S/N ratios, larger is better

Levels	A	B	C	D	E
1	7.4025	7.8289	7.5493	7.7731	7.6443
2	7.9017	7.4753	7.7548	7.6445	7.6597
Delta	0.4992	0.3536	0.2055	0.1286	0.0154
Rank	1	2	3	4	5

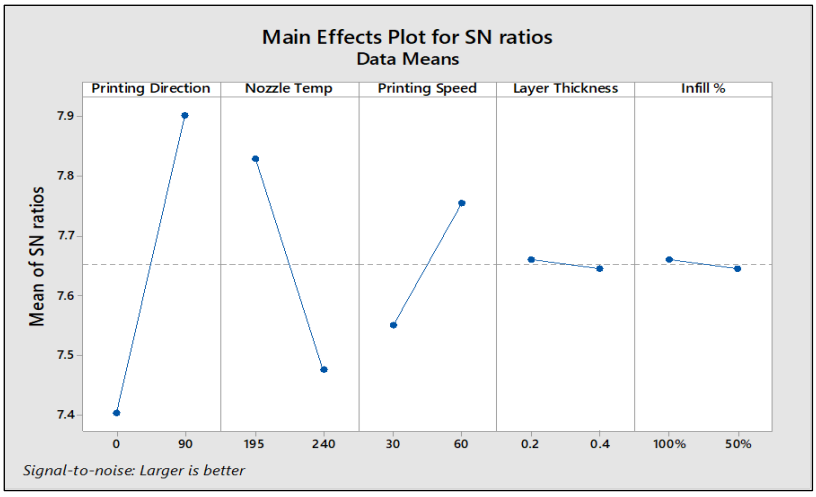

Fig. 13. Main effects plot for S/N ratios.

Table 9. ANOVA table for strength

Parameters	DOF	Sum of squares	Mean square	F-Value	P-Value	Contribution
A	1	0.0392	0.0392	46.12	0.021	55%
B	1	0.02	0.02	23.53	0.04	27%
C	1	0.0072	0.0072	8.47	0.101	8%
D	1	0.00005	0.00005	0.06	0.831	2%
E	1	0.00005	0.00005	0.06	0.831	2%
Error	2	0.0017	0.00085			
Total	7	0.0682				

https://doi.org/10.24191/jmeche.v23i1.457

It was demonstrated that two additional factors significantly impacted the 0° orientation since, as previously stated in Table 8, the 0° orientation is sensitive because the sample's width is greater than its height, as compared to the 90° orientation, giving the latter more strength. The trans-layer fusion bond is influenced by the nozzle temperature; at a lower temperature (195 °C), the bond is strong, and the material is strengthened due to the lower temperature difference and cooling effect. Additionally, the air gap is reduced, and the specimen's continuity is increased by increasing the infill percentage with 90° orientation; however, the tensile property of the 90° orientation may not be significantly impacted by an increase in infill density, as suggested by Chacón et al. (2017). Nozzle temperature and infill density have a complicated and unclear relationship. This intricacy makes it challenging to choose them all appropriately. Results also show that the strength increases with increased printing speed (60 mm/s). Fig 14 shows the interaction plot for strength analysis. The key interactions are as follows:

i. Printing Direction vs Nozzle Temperature
   - The lines diverge especially at higher temperatures.
   - This suggests a strong interaction: The effect of printing direction depends on nozzle temperature

ii. Printing Direction vs Printing Speed
   - Lines are not parallel, especially at speed 60 mm/s
   - Moderate interaction exists

iii. Nozzle Temperature vs Printing Speed
   - Line crosses, indicating a clear interaction.
   - The best speed setting may depend on the nozzle temperature.

iv. Layer thickness vs Infill Percentage
   - Lines cross over each other, suggesting a strong interaction.

v. Printing Direction vs Infill Percentage
   - Lines are not parallel, especially at 100% infill.
   - Suggest an interaction is present.

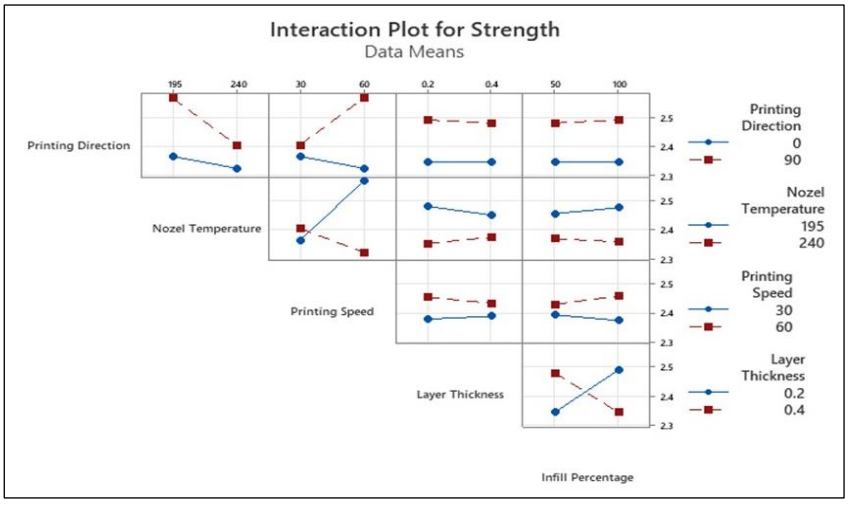

Fig. 14. Interaction plot for strength.

https://doi.org/10.24191/jmeche.v23i1.457

Based on these findings, it can be found that this configuration tallies with process configuration number 5, which offers the highest strength at 2.59 kN. As configuration five (5) had been tested (with 2.59 kN strength), no further verification experiment is needed.

CONCLUSION

This study aims to find the optimum process parameters that will give the maximum strength when tested on the 3D printing specimen specified. This study was conducted in line with the implementation of the Taguchi Design of Experiment method on a 3D-printed notched curved shell. 3D-printed samples of notched curve shells were printed using the Creality CR10S Pro-V2 printer. For a complete factorial experiment, 32 process parameters must be carried out. However, using the Taguchi method, the total number of experiments was reduced to eight (8), whereby three samples represented each process. Strength experiments were carried out, and it was found that configuration number five (5) yielded the highest strength of 2.59 kN. The "larger-the-better" equation was further confirmed using the Minitab software to plot the main effect for S/N ratios and analysis of variance (ANOVA). The results also show that the main contributing factors were printing direction (55%), nozzle temperature (27%), and printing speed (8%). Little contributions were from layer thickness and infill percentage. No verification experiment was needed as the output of the Minitab software tallies with the earlier experimental findings, whereby configuration no. 5 produced the highest strength of 2.59 kN. The objective of this study was met. Future recommendation is to study more of the significant process parameters interaction effects to better understand how these processes interact with one another during the 3D printing process.

ACKNOWLEDGEMENT

The authors would like to acknowledge and thank the College of Engineering, University Technology MARA, and Caidmark Sdn Bhd for their utmost support.

CONFLICT OF INTEREST STATEMENT

The authors agree that this research was conducted in the absence of any self-benefits, commercial or financial conflicts, and declare the absence of conflicting interests with the funders.

AUTHORS' CONTRIBUTIONS

The authors confirm their contribution to the paper as follows: study conception and design: Abdul Malik and Wahyu Kuntjoro; data collection: Abdul Malik ,Wahyu Kuntjoro, and Juri Saedon; analysis and interpretation of results: Abdul Malik, Wahyu Kuntjoro, and Juri Saedon; draft manuscript preparation: Abdul Malik, Wahyu Kuntjoro, Rizal Effendy, and Juri Saedon. All authors reviewed the results and approved the final version of the manuscript.

REFERENCES

Aloyaydi, B. A., Sivasankaran, S., & Ammar, H. R. (2019). Influence of infill density on microstructure

https://doi.org/10.24191/jmeche.v23i1.457

and flexural behavior of 3D printed PLA thermoplastic parts processed by fusion deposition modeling. AIMS Materials Science, 6(6), 1033–1048. https://doi.org/10.3934/matersci.2019.6.1033

Anitha, R., Arunachalam, S., & Radhakrishnan, P. (2001). Critical parameters influencing the quality of prototypes in fused deposition modelling. Journal of Materials Processing Technology, 118(1–3), 385–388. https://doi.org/10.1016/S0924-0136(01)00980-3

Athreya, S., & Venkatesh, Y. D. (2012). Application of Taguchi method for optimization of process parameters in improving the surface roughness of lathe facing operation. International Refereed Journal of Engineering and Science, 1(3), 13–19.

Bhavar, V., Kattire, P., Patil, V., Khot, S., Gujar, K., & Singh, R. (2017). A review on powder bed fusion technology of metal additive manufacturing. Additive Manufacturing Handbook. CRC Press.

Cariapa, V., Park, H., Kim, J., Cheng, C., & Evaristo, A. (2008). Development of a metal removal model using spherical ceramic media in a centrifugal disk mass finishing machine. International Journal of Advanced Manufacturing Technology, 39(1–2), 92–106. https://doi.org/10.1007/s00170-007-1195-5

Carlier, E., Marquette, S., Peerboom, C., Denis, L., Benali, S., Raquez, J. M., Amighi, K., & Goole, J. (2019). Investigation of the parameters used in fused deposition modeling of poly(lactic acid) to optimize 3D printing sessions. International Journal of Pharmaceutics, 565, 367–377. https://doi.org/10.1016/j.ijpharm.2019.05.008

Chacón, J. M., Caminero, M. A., García-Plaza, E., & Núñez, P. J. (2017). Additive manufacturing of PLA structures using fused deposition modelling: Effect of process parameters on mechanical properties and their optimal selection. Materials & Design, 124, 143–157. https://doi.org/10.1016/j.matdes.2017.03.065

Cho, E. E., Hein, H. H., Lynn, Z., Hla, S. J., & Tran, T. (2019). Investigation on influence of infill pattern and layer thickness on mechanical strength of PLA material in 3D printing technology. Journal of Engineering and Science Research, 3(2), 27–37. https://doi.org/10.26666/rmp.jesr.2019.2.5

Chohan, J. S., & Singh, R. (2017). Pre and post processing techniques to improve surface characteristics of FDM parts: a state of art review and future applications. Rapid Prototyping Journal, 23(3), 495–513. https://doi.org/10.1108/RPJ-05-2015-0059

Dave, H. K., Prajapati, A. R., Rajpurohit, S. R., Patadiya, N. H., & Raval, H. K. (2022). Investigation on tensile strength and failure modes of FDM printed part using in-house fabricated PLA filament. Advances in Materials and Processing Technologies, 8(1), 576–597. https://doi.org/10.1080/2374068X.2020.1829951

Dev, S., & Srivastava, R. (2020). Experimental investigation and optimization of FDM process parameters for material and mechanical strength. Materials Today: Proceedings, 26(2), 1995–1999. https://doi.org/10.1016/j.matpr.2020.02.435

El Magri, A., El Mabrouk, K., Vaudreuil, S., & Ebn Touhami, M. (2020). Experimental investigation and optimization of printing parameters of 3D printed polyphenylene sulfide through response surface methodology. Journal of Applied Polymer Science, 138(1), 1–13. https://doi.org/10.1002/app.49625

Guduru, K. K., & Srinivasu, G. (2020). Effect of post treatment on tensile properties of carbon reinforced PLA composite by 3D printing. Materials Today: Proceedings, 33(8), 5403–5407. https://doi.org/10.1016/j.matpr.2020.03.128

Hikmat, M., Rostam, S., & Ahmed, Y. M. (2021). Investigation of tensile property-based Taguchi method of PLA parts fabricated by FDM 3D printing technology. Results in Engineering, 11, 100264.

https://doi.org/10.24191/jmeche.v23i1.457

https://doi.org/10.1016/j.rineng.2021.100264

Iljaszewicz, P., Lusiak, T., Pastuszak, A., & Novak, A. (2020). Aerodynamic analysis of the aircraft model made with the 3D printing method. Transportation Research Procedia, 51, 118–133. https://doi.org/10.1016/j.trpro.2020.11.014

İriç, S. (2020). Experimental investigation on effect to the specific strength of FDM fabrication parameters using Taguchi method. Sakarya Univeristy Journal of Science, 24(5), 984-990. https://doi.org/10.16984/saufenbilder.771389

Kim, Y., & Park, J. (2020). A theory for the free vibration of a laminated composite rectangular plate with holes in aerospace applications. Composite Structures, 251, 112571. https://doi.org/10.1016/j.compstruct.2020.112571

Kumar, R., & Kumar, S. (2020). Trending applications of 3D printing: a study. Asian Journal of Engineering and Applied Technology, 9(1), 1–12. https://doi.org/10.51983/ajeat-2020.9.1.1085

Kun, K. (2016). Reconstruction and development of a 3D printer using FDM technology. Procedia Engineering, 149, 203–211. https://doi.org/10.1016/j.proeng.2016.06.657

Kuntjoro, W., Abdul Jalil, A. M. H., Ahmad Redzuan, A. N., & Mohd Nasir, R. E. (2023a). Parametric study on the stress behaviour of 3D printed PLA plate with hole. AIP Conference Proceedings, 2847(1), 050009. https://doi.org/10.1063/5.0166040

Kuntjoro, W., Abdul Jalil, A. M. H., Ahmad Redzuan, A., & Mohd Nasir, R. E. (2023b). Stress behaviour of 3D printed plate with hole. Journal of Engineering and Technological Advances, 8(1), 13-29. https://doi.org/10.35934/segi.v8i1.58

Kuntjoro, W., Latip, U. H. M., Mohd Nasir, R. E., & Ramly, R. (2022a). Static analysis of 3D-printed sub wing box lug joint assembly using finite element method. Journal of Aeronautics, Astronautics and Aviation, 54(3), 335–346. https://doi.org/10.6125/JoAAA.202209_54(3).10

Kuntjoro, W., Ridhwan, M. A. M., Mohd Nasir, R. E., & Muta'ali, A. B. A. (2022b). Structural analysis of 3D printed UAV straight wing box. Journal of Aeronautics, Astronautics and Aviation, 54(3), 347–356. https://doi.org/10.6125/JoAAA.202209_54(3).11

Liu, L., Shamir, A., Wang, C., & Whitening, E. (2014). 3D printing oriented design: geometry and optimization. Conference of SIGGRAPH Asia 2014 Courses (p. 1). Association for Computing Machinery. https://doi.org/10.1145/2659467.2675050

Mannoor, M. S., Jiang, Z., James, T., Kong, Y. L., Malatesta, K. A., Soboyejo, W. O., Verma, N., Gracias, D. H., & McAlpine, M. C. (2013). 3D printed bionic ears. Nano Letters, 13(6), 2634–2639. https://doi.org/10.1021/nl4007744

Michaels, D. (2017). GE, rivals turn to Europe for push into 3D printing. https://www.foxbusiness.com/features/ge-rivals-turn-to-europe-for-push-into-3-d-printing-wsj

Mo, J. P. T., Cheung, S. C. P., & Das, R. (2019). Chapter 11 - Thin plate deflection. Demystifying Numerical Models (pp. 235–255). Elsevier. https://doi.org/10.1016/b978-0-08-100975-8.00011-4

Mohamed, O. A., Masood, S. H., & Bhowmik, J. L. (2015). Optimization of fused deposition modelling process parameters: a review of current research and future prospects. Advances in Manufacturing, 3(1), 42–53. https://doi.org/10.1007/s40436-014-0097-7

Munprom, R., & Limtasiri, S. (2019). Optimization of stereolithographic 3D printing parameters using

Taguchi method for improvement in mechanical properties. Materials Today: Proceedings, 17(4), 1768–1773. https://doi.org/10.1016/j.matpr.2019.06.209

Muta'ali, A. B. A., Nasir, R. E. M., Wisnoe, W., & Kuntjoro, W. (2020). Aerodynamic performance of a tail-less blended wing-body small transport aircraft. Journal of Advanced Research in Fluid Mechanics and Thermal Sciences, 66(1), 135–150.

Ngo, T. D., Kashani, A., Imbalzano, G., Nguyen, K. T. Q., & Hui, D. (2018). Additive manufacturing (3D printing): a review of materials, methods, applications and challenges. Composites Part B: Engineering, 143, 172–196. https://doi.org/10.1016/j.compositesb.2018.02.012

Nguyen, D. T., Meyers, C., Yee, T. D., Dudukovic, N. A., Destino, J. F., Zhu, C., Duoss, E. B., Baumann, T. F., Suratwala, T., Smay, J. E., & Dylla-Spears, R. (2017). 3D-printed transparent glass. Advanced Materials, 29(26), 1–5. https://doi.org/10.1002/adma.201701181

Pukale, B., & Reddy, M. A. (2014). Stress analysis and damage tolerance evaluation for wing structure with a large cutout in the bottom skin. International Journal of Engineering Technology and Sciences, 2(1), 33–38. https://doi.org/10.15282/ijets.2.2014.1.7.1014

Raj, S. A., Muthukumaran, E., & Jayakrishna, K. (2018). A case study of 3D printed PLA and its mechanical properties. Materials Today: Proceedings, 5(5), 11219–11226. https://doi.org/10.1016/j.matpr.2018.01.146

Rao, R. S., Kumar, C. G., Prakasham, R. S., & Hobbs, P. J. (2008). The Taguchi methodology as a statistical tool for biotechnological applications: a critical appraisal. Biotechnology Journal, 3(4), 510–523. https://doi.org/10.1002/biot.200700201

Reuters (2017). 3D printing titanium parts could save boeing millions on dreamliner production. https://fortune.com/2017/04/11/3d-printing-norsk-boeing-dreamliner/

Saedon, J. B., Jaafar, N., Nor, N. H. M., Yahaya, M. A., & Husain, H. (2015). Multi-objective optimization in wire-electrical discharge machining (WEDM) of titanium alloy. Jurnal Teknologi, 76(6), 31–35. https://doi.org/10.11113/jt.v76.5670

Schiavone, N., Verney, V., & Askanian, H. (2020). Effect of 3D printing temperature profile on polymer materials behavior. 3D Printing and Additive Manufacturing, 7(6), 311–325. https://doi.org/10.1089/3dp.2020.0175

Sheoran, A. J., & Kumar, H. (2020). Fused Deposition modeling process parameters optimization and effect on mechanical properties and part quality: review and reflection on present research. Materials Today: Proceedings, 21(3), 1659–1672. https://doi.org/10.1016/j.matpr.2019.11.296

Siraj, I., & Bharti, P. S. (2020). Reliability analysis of a 3D Printing process. Procedia Computer Science, 173, 191–200. https://doi.org/10.1016/j.procs.2020.06.023

Sundaresan, M. J., Ghoshal, A., Li, J., Schulz, M. J., Pai, P. F., & Chung, J. H. (2003). Experimental damage detection on a wing panel using vibration deflection shapes. Structural Health Monitoring, 2(3), 243–256. https://doi.org/10.1177/1475921703036047

Suteja, T. J., & Soesanti, A. (2020). Mechanical properties of 3D printed polylactic acid product for various infill design parameters: a review. Journal of Physics: Conference Series, 1569, 042010. https://doi.org/10.1088/1742-6596/1569/4/042010

Tong, Q., Xue, K., Wang, T., & Yao, S. (2020). Laser sintering and invalidating composite scan for improving tensile strength and accuracy of SLS parts. Journal of Manufacturing Processes, 56, 1–11.

https://doi.org/10.24191/jmeche.v23i1.457

https://doi.org/10.1016/j.jmapro.2020.04.056

Yadav, D., Chhabra, D., Gupta, R. K., Phogat, A., & Ahlawat, A. (2020). Modeling and analysis of significant process parameters of FDM 3D printer using ANFIS. Materials Today: Proceedings, 21(3), 1592–1604. https://doi.org/10.1016/j.matpr.2019.11.227

Yao, T., Deng, Z., Zhang, K., & Li, S. (2019). A method to predict the ultimate tensile strength of 3D printing polylactic acid (PLA) materials with different printing orientations. Composites Part B: Engineering, 163, 393–402. https://doi.org/10.1016/j.compositesb.2019.01.025

Yao, T., Ye, J., Deng, Z., Zhang, K., Ma, Y., & Ouyang, H. (2020). Tensile failure strength and separation angle of FDM 3D printing PLA material: Experimental and theoretical analyses. Composites Part B: Engineering, 188, 107894. https://doi.org/10.1016/j.compositesb.2020.107894

Zheng, Y., He, Z. Z., Yang, J., & Liu, J. (2014a). Personal electronics printing via tapping mode composite liquid metal ink delivery and adhesion mechanism. Scientific Reports, 4, 4588. https://doi.org/10.1038/srep04588

Zheng, X., Lee, H., Weisgraber, T. H., Shusteff, M., Deotte, J., Duoss, E. B., Kuntz, J. D., Biener, M. M., Ge, Q., Jackson, J. A., Kucheyev, S. O., Fang, N. X., & Spadaccini, C. M. (2014b). Ultralight, ultrastiff mechanical metamaterials. Science, 344(6190), 1373–1377. https://doi.org/10.1126/science.1252291

https://doi.org/10.24191/jmeche.v23i1.457